Modeling of Motor Bearing Currents in PWM Inverter Drives

Shaotang Chen, *Member, IEEE,* Thomas A. Lipo, *Fellow, IEEE,* and Dennis Fitzgerald

***Abstract*— Pulsewidth modulated (PWM) inverters have recently been found to be a major cause of motor bearing failures in inverter-motor drive systems. Specifically, all inverters generate common mode voltages relative to the earth ground. The voltages provide coupling or bearing currents through motor parasitic capacitances to the rotor iron which flow via the bearings to the grounded stator case.**

In this paper, a model of bearing currents caused by PWM inverter is proposed. The model is based on transmission line theory which uses an equivalent lumped parameter π-network to describe the parasitic coupling phenomenon. The model parameters are then identified by matching the calculated model outputs with those of experimental measurement. The validation of the method is demonstrated by the fact that the model can reproduce a variety of experimental results obtained on a test motor.

An application of this method also gives a motor grounding current model. As the conducted electromagnetic interference (EMI) in drive systems is related to the grounding currents, the grounding current model can be used for the analysis of conducted EMI in motor-drive systems.

***Index Terms*—Bearing current, bearing damage, bearing failures, induction motor, parasitic capacitive coupling, PWM inverter, shaft voltage, common mode voltage**

I. Introduction

RECENTLY, pulsewidth modulated (PWM) inverters have been found to be a major cause of motor bearing failures in inverter-motor drive systems [1]–[3]. In principle, all inverters generate common mode voltages relative to the earth ground which provide coupling currents through the motor parasitic capacitances to the rotor iron. As the coupling currents find their way via the motor bearings back to the grounded stator case, they form the so-called bearing currents [2], [3].

The principle of bearing current generation can be illustrated using Fig. 1. By taking the inverter negative dc bus, O, as a reference for common mode voltages, the common mode voltage at motor phase A input terminal is V_{AO}. The parasitic coupling capacitances from the motor windings to the stator and rotor irons are represented by $C_{\rm ws}$ and $C_{\rm wr}$, respectively. There is also a capacitance C_g present across the bearings

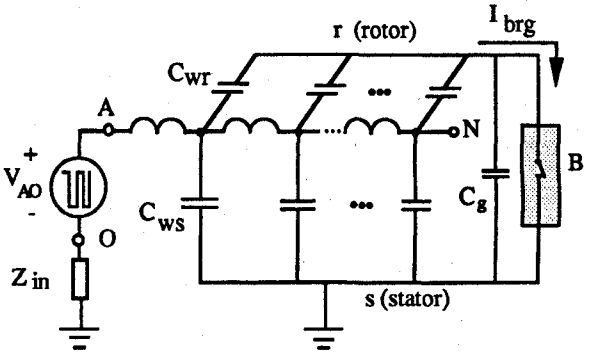

Fig. 1. Principle of bearing current generation in inverter-motor system.

which mainly consists of the motor air gap capacitance. The bearings are approximated by a switch B which turns on and off randomly based on observation of electric behavior of motor rotating bearings [1], [2]. A closed-loop parasitic coupling circuit is formed if the coupling capacitance from the negative dc bus to the earth is also recognized. This capacitance is represented by an impedance $Z_{\rm in}$ which will be treated as the internal impedance of the common mode voltage source V_{AO}. Based on the above circuit, a bearing current $I_{\rm brg}$ is easily identified as the total current flowing into all $C_{\rm wr}$'s and then via bearing model B back to the grounded stator. Similarly, for phases B and C, common mode voltages V_{BO} and V_{CO} also contribute to the bearing current.

The distributed parameter circuit in Fig. 1 is, however, not suitable for a simplified analysis of the bearing currents. Equivalent lumped parameter circuit models are developed in this paper to describe the parasitic coupling phenomenon. In principle, the parasitic coupling circuits are the same as transmission line circuits. Based on transmission line theory, a distributed parameter circuit can be modeled by an equivalent lumped parameter π-network which gives the same input and output relationship. The method is applied to give a model of coupling from motor windings to stator irons—the motor grounding current model, and a model of coupling from motor windings to the rotor irons—the bearing current model. The model parameters are then identified by matching the calculated model outputs with those of experimental measurement. The validation of the modeling is demonstrated by the fact that the models can reproduce a variety of experimental results obtained on the test motor. Therefore, the proposed models can be used to analyze the effect of bearing currents and facilitate the determination of solutions to suppress these currents. As the motor grounding current is a major source of conducted electromagnetic interference (EMI) in inverter-motor systems,

Paper IPCSD 96–30, approved by the Industrial Drives Committee of the IEEE Industry Applications Society for presentation at the 1995 IEEE Industry Applications Society Annual Meeting, Lake Buena Vista, FL, October 8–12. Manuscript released for publication April 22, 1996.

S. Chen is with the GM Research & Development Center, Warren, MI 48090 USA.

T. A. Lipo is with the Department of Electrical and Computer Engineering, University of Wisconsin, Madison, WI 53706–1691 USA.

D. Fitzgerald is with the Motion Control Division, Yaskawa Electric America Inc., Northbrook, IL 60062–2028 USA.

Publisher Item Identifier S 0093-9994(96)06638-8.

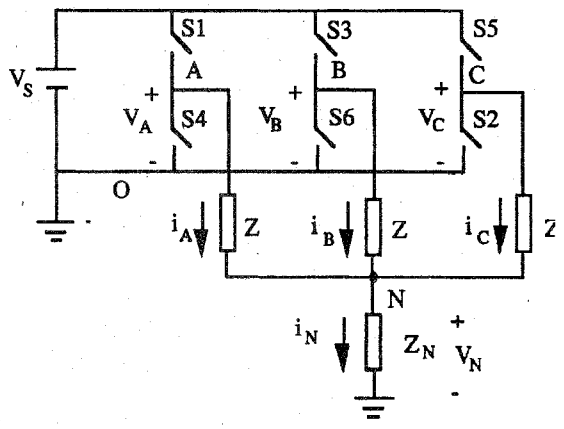

Fig. 2. Three-phase inverter-load system including common mode impedance Z_n.

the motor grounding current model can thus be applied to the analysis of conducted EMI in motor-drive systems.

II. Common Mode Excitation and Response

For a balanced three-phase inverter-load system shown in Fig. 2, the three-phase load is represented by Z. Assume that the zero sequence impedance of the load is Z_O and that there exists a common mode impedance Z_N from the neutral point N to the ground. Due to existence of common mode excitations, such a system must contain both differential mode and common mode responses. While the differential mode response has been well known as the three-phase input and output relationship, the common mode response has not yet been formally established. The purpose of Section II is to derive a common mode circuit model which describes only the common mode response of the system.

In general, for any three-phase load Z, the zero sequence voltage and current are defined by

$$V_O = \frac{V_{AN} + V_{BN} + V_{CN}}{3} = \frac{V_A + V_B + V_C}{3} - V_N \quad (1)$$

and

$$i_O = \frac{i_A + i_B + i_C}{3} \quad (2)$$

respectively. The relationship between zero sequence voltage and current is governed by

$$V_O = i_O Z_O. \quad (3)$$

Based on (1)–(3), the common mode current, i_N, and the common mode voltage at neutral point, V_N, can be derived as

$$i_N = i_A + i_B + i_C = 3i_O = \frac{3}{Z_O + 3Z_N}\frac{V_A + V_B + V_C}{3} \quad (4)$$

and

$$V_N = \frac{3Z_N}{Z_O + 3Z_N}\frac{V_A + V_B + V_C}{3}. \quad (5)$$

It is interesting to notice that the three-phase balanced impedance Z does not appear in (4) and (5). This implies that the common mode circuit can be decoupled from the differential mode circuit in a balanced three-phase system.

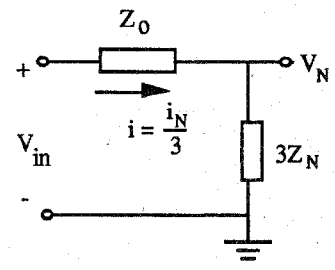

Fig. 3. Model of common mode excitation.

Since only the zero sequence impedance of the three-phase load Z is common to all three phases, it is reasonable that Z_O, instead of Z, will appear in the common mode equations (4) and (5).

As the common mode voltage V_N and common mode current i_N are the only physically meaningful common mode outputs in the system, a model of common mode excitation can be readily obtained based on (4) and (5). By defining an equivalent common mode voltage input

$$V_{\text{in}} = \frac{V_A + V_B + V_C}{3} \quad (6)$$

the common mode model can be simply represented by Fig. 3.

III. Modeling of Coupling from Windings to Stator—Motor Grounding Currents

The coupling between the motor windings and the rotor is much less than the coupling between the same windings and the stator. The modeling will use this fact and only consider the coupling between the windings and the stator. A distributed circuit model of coupling between the stator windings and the stator can be represented by Fig. 4. In Fig. 4, Z denotes the impedance per unit length of motor phase windings, and Z_{ws} the per unit length windings to stator parasitic coupling impedance which is mainly capacitive. Due to symmetric design of motor structures, a uniform distribution of parasitic coupling impedances is assumed. This assumption will apply to parasitic couplings from the windings to both the stator and the rotor.

Theoretically, the circuit represents a three-phase transmission line with one of its terminations shorted as the winding neutral N. As is treated in transmission line theory, if only the input and output characteristics are of interest, an equivalent π-network can be used to describe the input and output relationship. In other words, for each phase, the distributed parameter circuit can be replaced by an equivalent π-network. By adding all three parallel connected neutral to ground impedances, an equivalent lumped parameter circuit model is obtained as shown in Fig. 5. In this model, $V_N$is the voltage of motor neutral point and I_{ws} is the total coupling current from the windings to the stator. All parameters in the model are to be determined which are functions of Z and Z_{ws}.

Based on the derivation in Section II, a simplified model of common mode excitation can be drawn as shown in Fig. 6 where L_o, C_o, and R_o are the zero sequence components contained in L_s, C_s, and R_s of Fig. 5. As the voltage of the motor neutral point and the total coupling current from the

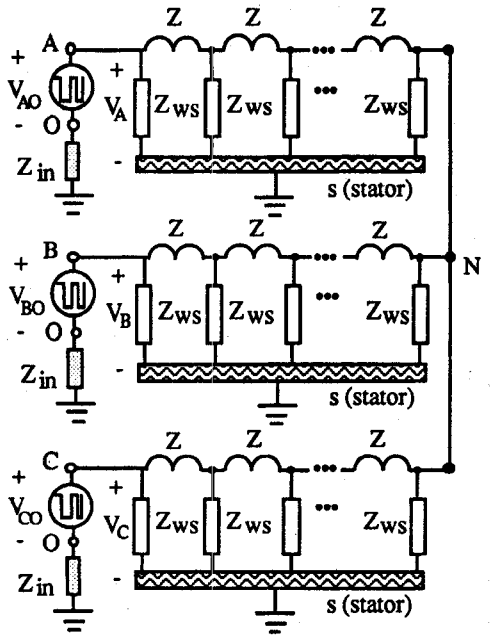

Fig. 4. Distributed circuit representation of coupling from motor windings to stator laminations.

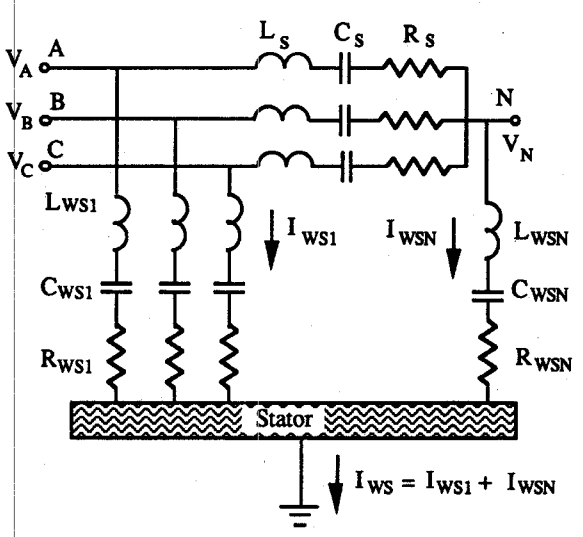

Fig. 5. An equivalent lumped parameter circuit showing coupling from motor windings to stator iron laminations.

windings to the stator are of interest, their relationship to the common mode input voltage V_{in} can be determined as

$$\frac{V_N}{V_{\text{in}}} = \frac{3Z_{\text{WSN}}}{Z_O + 3Z_{\text{WSN}}} \tag{7}$$

and

$$\frac{i_{\text{ws}}}{V_{\text{in}}} = \frac{3}{Z_{\text{WS1}}} + \frac{3}{Z_O + 3Z_{\text{WSN}}} \tag{8}$$

where Z_O, Z_{WS1} and Z_{WSN} represent $(L_O,\ C_O,\ R_O)$, $(L_{\text{WS1}},\ C_{\text{WS1}},\ R_{\text{WS1}})$, and $(L_{\text{WSN}},\ C_{\text{WSN}},\ R_{\text{WSN}})$, respectively.

It is obvious that the V_N is not related to impedance Z_{WS1}. For coupling currents, simulation based on the model shows that I_{WS1} is much larger than I_{WSN}. Therefore, the grounding

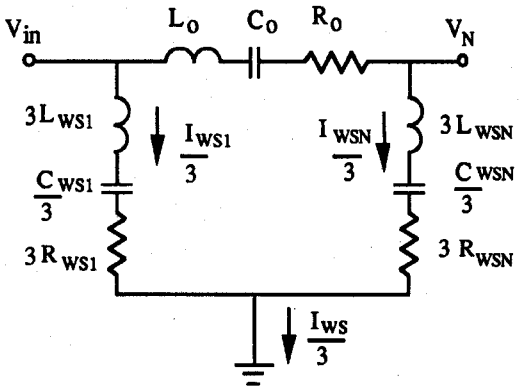

Fig. 6. Model of common mode coupling from windings to stator laminations.

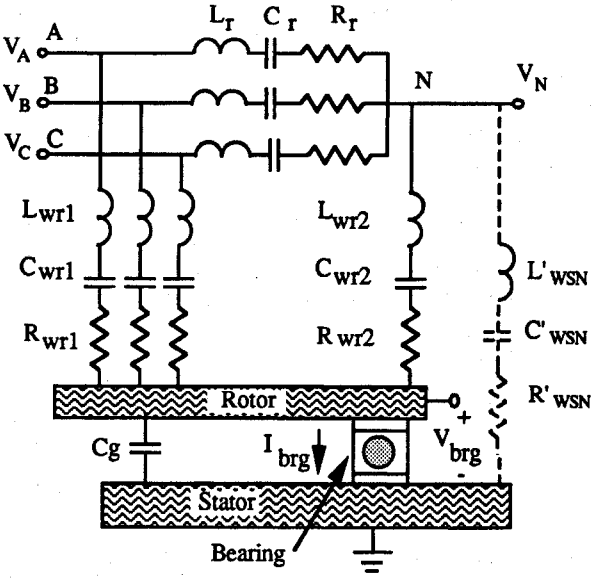

Fig. 7. Lumped parameter equivalent circuit of coupling from stator windings to rotor iron laminations.

current I_{WS} is primarily determined by Z_{WS1}, while the motor winding neutral point voltage is governed by Z_{WSN}.

IV. Modeling of Coupling from Windings to Rotor—Bearing Current Model

Bearing currents are only related to the common mode coupling between the windings and the rotor and are not represented in the circuit of Fig. 6. However, as both coupling currents to rotor and stator share the same path of the stator windings and the stator coupling currents are significant, the influence of stator coupling currents to the bearing current model should be taken into account.

In spite of the above statement, let us first ignore for the moment the flow of stator coupling currents in the windings. Similar to Section III, the same distributed parameter circuit model of motor windings as shown in Fig. 4 can also be used to describe the coupling from the same windings to the rotor except that Z_{ws} has to be replaced by Z_{wr}. Also, in terms of input and output relationship, the rotor coupling circuit can be represented by an equivalent lumped π-network. A rotor

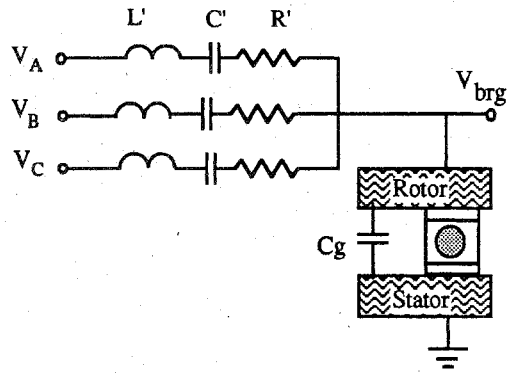

Fig. 8. Simplified rotor coupling model ignoring influence of stator coupling currents.

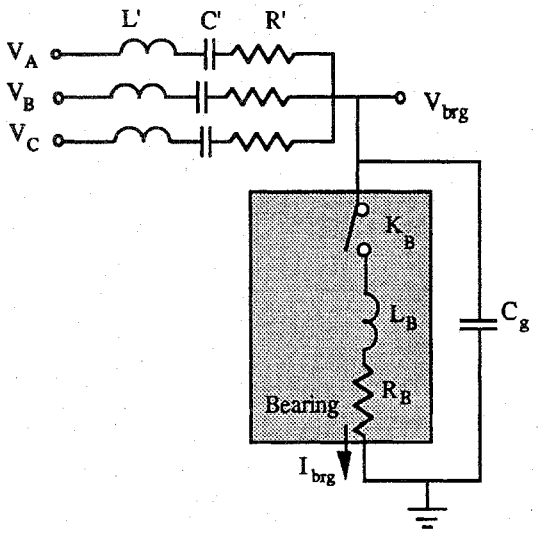

Fig. 9. Combination of bearing model to rotor coupling circuit.

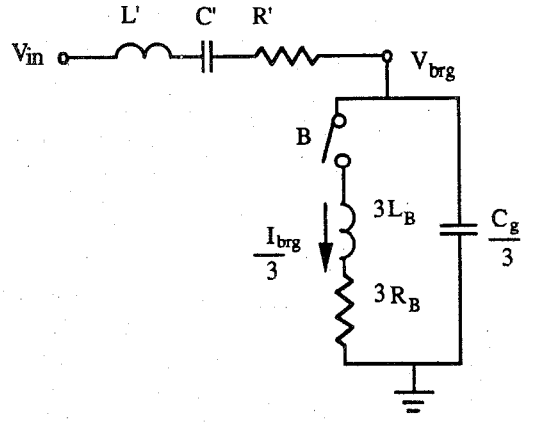

Fig. 10. Simplified bearing current model.

coupling model together with an illustrated bearing block is then depicted in Fig. 7.

Now, it is useful to consider the effect of stator coupling currents in the same windings. The equivalence of stator coupling currents is an impedance Z'_{WS1} connected from the input of each phase winding to the stator and an impedance Z'_{WSN} connected from the neutral point to the stator as shown

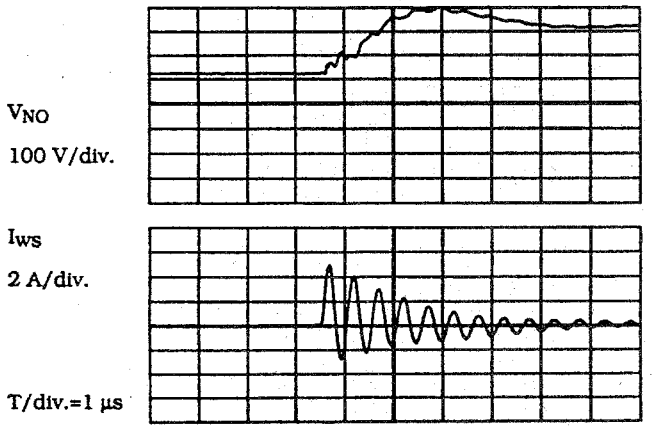

(a)

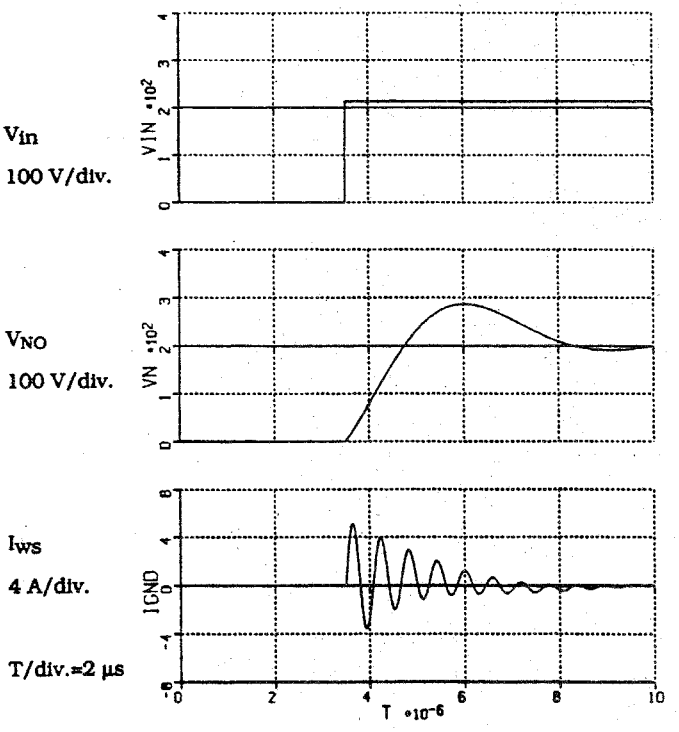

(b)

Fig. 11. Comparison of measured and simulated motor neutral voltage and grounding currents. (a) Measured response of V_N and I_{ws} to a step V_{in}. (b) Calculated response of V_N and I_{ws} to a step V_{in}.

in Fig. 5. It is apparent that Z'_{WS1} will have no influence on bearing currents and voltages, while Z'_{WSN} represents those stator coupling currents which have an effect on the rotor coupling circuit. Therefore, the influence of stator coupling currents to the rotor coupling path can always be considered by adding an impedance L'_{WSN}, C'_{WSN} and R'_{WSN} to the circuit model as is indicated by the dashed line portion in Fig. 7. Notice that Z'_{WSN} and Z_{WSN} may not be the same.

The uncertainty of the value Z'_{WSN} will definitely cause a small error in the calculation of the bearing current i_{brg} and the shaft voltage V_{brg} as was observed in our simulation study. However, to simplify the analysis, we will neglect the influence of Z'_{WSN}. However, In case precise modeling of bearing currents is required, Z'_{WSN} can be readily added into the rotor coupling model as shown in Fig. 7.

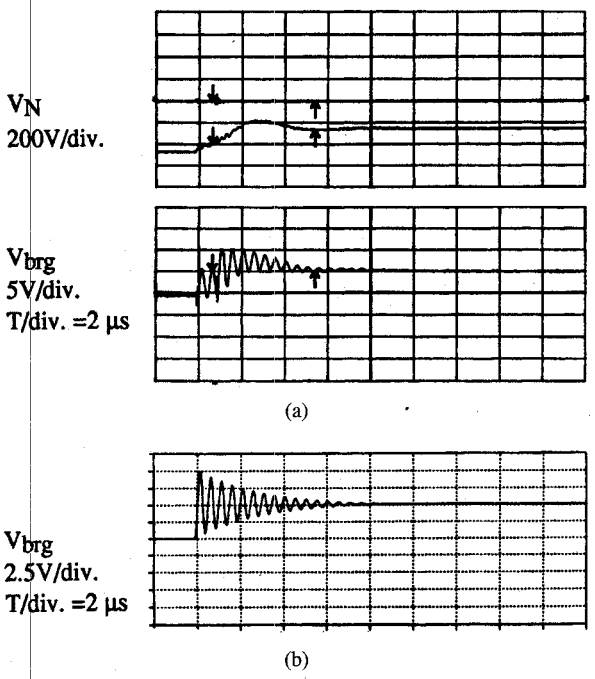

Fig. 12. Comparison of measured and simulated bearing voltages. (a) Measured neutral point and shaft voltage waveforms. (b) Simulated shaft voltages under same excitation condition.

TABLE I
IDENTIFIED PARAMETERS OF STATOR COUPLING MODEL

$L_o = 500\,\mu H$	$C_o = 500$ nF	$R_o = 100$ ohms
$L_n = 10$ nH	$C_n = 5$ nF	$R_n = 100$ ohms
$L_1 = 11\,\mu H$	$C_1 = 800$ pF	$R_1 = 15$ ohms

TABLE II
IDENTIFIED PARAMETERS OF BEARING CURRENT MODEL

$L' = 300\mu H$	$C' = 20$ pF	$R' = 200$ ohms
$L_B = 150$ nH	$C_g = 800$ pF	$R_B = 6.5$ ohms

By ignoring Z'_{WSN}, the circuit model shown in Fig. 7 can be simplified by replacing the π-network with a single $L'C'R'$ component as shown in Fig. 8. The bearing model can then be combined with the coupling circuit which results in the circuit shown in Fig. 9. The bearings are modeled as a switch B with certain internal inductance L_B and resistance R_B.

Finally, as the common mode outputs always depend on the equivalent common mode excitation V_{in} instead of V_A, V_B, and V_C separately, the model shown in the Fig. 9 can be further simplified to the bearing current model shown in Fig. 10.

V. SIMULATION AND EXPERIMENTAL VERIFICATION OF THE MODELS

With the above models, system identification procedures can now be initiated to determine all of the parameters of each model. Given an initial guess of parameters, the models shown in Figs. 6 and 10 are used to calculate the output variables. The results are then compared with experimental measurement until a set of optimal parameters is found. To avoid the uncertainty of dealing with the ground path impedance of the common mode, the motor case has been connected to the negative dc bus (as voltage reference) which forces the equivalent common mode voltage internal impedance to equal zero. In this configuration, an experimental measurement of the neutral point voltage and grounding cable current (neglecting the contribution of bearing currents) waveforms are shown in Fig. 11(a). With the parameters listed in Table I, the calculation results based on the stator coupling model of Fig. 6 are plotted in Fig. 11(b). By comparing Fig. 11(a) and (b), it is seen that the waveforms are almost identical. Therefore, it is apparent that the parameters can be identified satisfactorily in this manner.

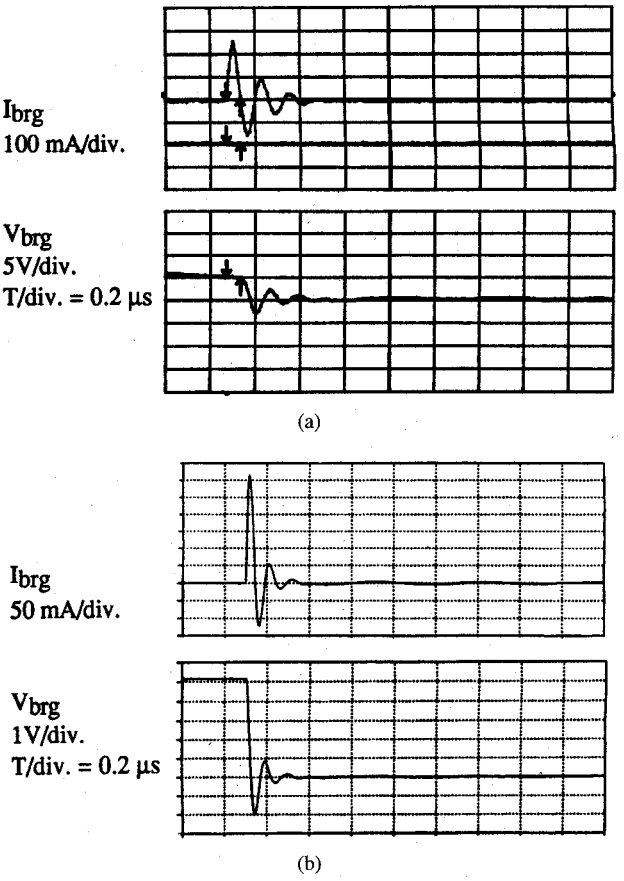

Fig. 13. Bearing current spike caused by discharge of airgap capacitor. (a) Measured bearing current spike and shaft voltage, (b) Calculated bearing current spike and shaft voltage.

Similar system identification procedures have been performed to determine the parameters of the bearing current model. The identification is based on the experimental measurement of responses of bearing voltages V_{brg} and currents I_{brg} to the common mode excitation. For a step input of common mode voltage V_{in}, a plot of the experimental measured bearing voltage V_{brg} is shown in Fig. 12(a). As the bearing voltage is seen to charge up during each inverter switching, it is apparent that switch B in the bearing model must be open. Therefore, based on the waveforms and the corresponding circuit model, parameters L', C', R', and C_g can be identified. Fig. 12(b) shows a simulated response based on the model of Fig. 9 and the identified parameters listed in Table II. The identification of L_B and R_B is based on Fig. 13(a) which shows a current spike produced by the discharge of the airgap capacitor C_g after switch B is closed.

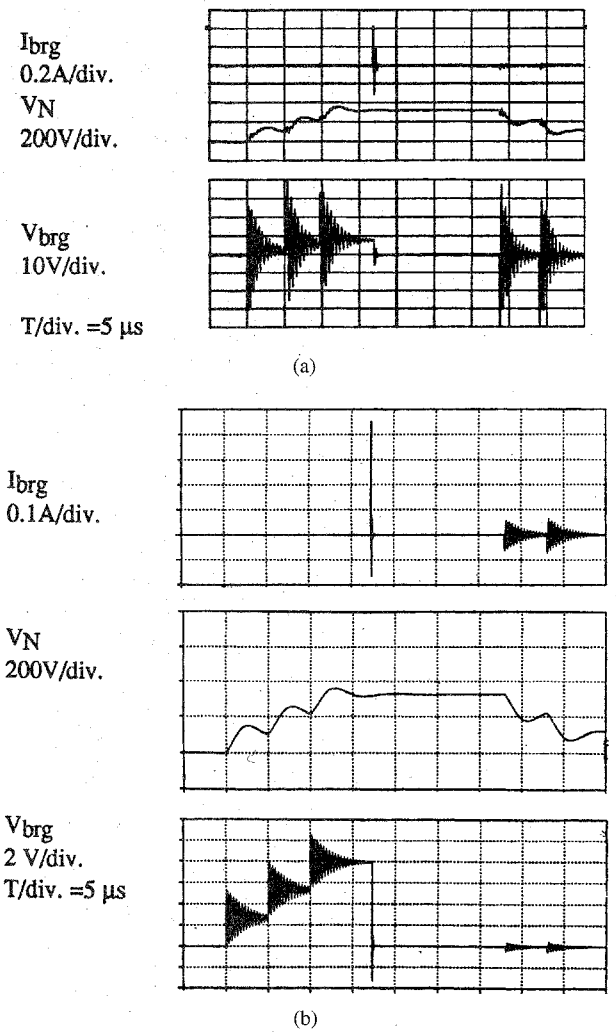

Fig. 14. Process of bearing current and shaft voltage generation: (a) Experimental observation of bearing current generation. (b) Simulation of bearing current generation.

Based on the identified parameters in Tables I and II, simulations have been performed to compare with numerous other experimental results. Fig. 14 shows one of the important results. In Fig. 14, the motor neutral point voltage is seen to increase step by step which corresponds to similar step-up in common mode voltage excitation V_{in} caused by PWM switching in the inverter. The bearing or shaft voltage V_{brg} follows the pattern of the motor neutral point voltage. This behavior is due to the capacitor divider effect of C_g and C_{wr}'s. The measured bearing current during the shaft voltage charge-up is seen to be almost zero due to high impedance inside the bearings. However, an abrupt voltage drop in bearing voltage accompanied by a large bearing current spike is observed which is actually caused by the sudden short circuit behavior inside the bearings. After bearings become short-circuited, some dv/dt related bearing currents begin to appear. By comparing the experimental measurement with the simulation traces in Fig. 14, it is seen that the results are almost identical except the difference in bearing voltage ringing during the transient which is believed to be caused mainly by instrumentation error. Therefore, the bearing current and motor grounding current models are clearly able to properly describe the bearing current and grounding current phenomena in inverter drives.

VI. Conclusion

This paper briefly discusses the mechanism of bearing current generated by PWM inverters which is related to the common mode voltages and parasitic capacitive couplings. Equivalent lumped parameter circuit models have been derived to describe the coupling from the windings to the stator and the rotor, respectively. Simulation is then performed to identify the model parameters by matching the simulated results with those of experimental measurement. The bearing current model and stator coupling model are shown to be able to predict the motor bearing currents and the grounding currents, respectively. Comparison of the predicted results with experimental measurements on a specially equipped motor shows good agreement. The bearing current model should prove useful for understanding of the phenomenon and for assisting in the determination of a feasible solution to the problem. The motor grounding current model can also be applied to the analysis of conducted EMI generation in motor-inverter systems.

References

[1] J. Erdman, R. J. Kerkman, D. Schlegel, and G. Skibinski, "Effect of PWM inverters on AC motor bearing currents and shaft voltages," in *IEEE, APEC-95, 10th Annual Applied Power Electronics Conference and Exposition*, Mar. 5–9, 1995, vol. 1, pp. 24–33.

[2] S. Chen, T. A. Lipo, and D. Fitzgerald, "Source of induction motor bearing currents caused by PWM inverters," *IEEE Trans. Energy Conversion*, vol. 11, pp. 25–32, Mar. 1996.

[3] S. Chen, "Bearing current, EMI and soft switching in induction motor drives—A systematic analysis, design and evaluation," Ph.D. dissertation, Univ. Wisconsin, Madison, 1995.

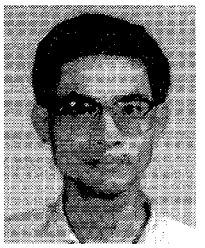

Shaotang Chen (S'93–M'96) received the B.Eng. and the M.Eng. degrees from the Central China University of Science and Technology, Wuhan, in 1983 and 1986, respectively, and the M.S. and the Ph.D. degrees from the University of Wisconsin, Madison, in 1993 and 1995, respectively.

He was with the Central China University of Science and Technology, Wuhan, China, from 1986 to 1991, and is currently with the Research and Development Center, General Motors, Warren, MI. His research interests are in control of electric machines, electric machine drives, and power electronics.

Thomas A. Lipo (M'64–SM'71–F'87), for a photograph and biography, see this issue, p. 1337.

Dennis Fitzgerald received the B.S. degree in marine engineering from the United States Merchant Marine Academy, Kings Point, NY.

He is the General Manager of the Motion Control Division, Yaskawa Electric America Inc., Northbrook, IL. Before joining Yaskawa, he was Product Marketing Manager for MagneTek, New Berlin, WI. MagneTek is one of Yaskawa's business partners for Yaskawa Inverter sales.